

Design of Wind Turbine Torque Controller with Second-Order Integral Sliding Mode Based on VGWO Algorithm

MA Leiming¹, XIAO Lingfei^{1*}, SATTAROV Robert R², HUANG Xinhao¹

1. College of Energy and Power Engineering, Nanjing University of Aeronautics and Astronautics,
Nanjing 210016, P. R. China;

2. Department of Electromechanics, Ufa State Aviation Technical University, Ufa, Russia

(Received 9 March 2020; revised 16 September 2020; accepted 1 December 2020)

Abstract: A robust control strategy using the second-order integral sliding mode control (SOISM) based on the variable speed grey wolf optimization (VGWO) is proposed. The aim is to maximize the wind power extraction of wind turbine. Firstly, according to the uncertainty model of wind turbine, a SOISM torque controller with fast convergence speed, strong robustness and effective chattering reduction is designed, which ensures that the torque controller can effectively track the reference speed. Secondly, given the strong local search ability of the grey wolf optimization (GWO) and the fast convergence speed and strong global search ability of the particle swarm optimization (PSO), the speed component of PSO is introduced into GWO, and VGWO with fast convergence speed, high solution accuracy and strong global search ability is used to optimize the parameters of wind turbine torque controller. Finally, the simulation is implemented based on Simulink/SimPowerSystem. The results demonstrate the effectiveness of the proposed strategy under both external disturbance and model uncertainty.

Key words: integral sliding mode; second-order sliding mode; maximum power point tracking; optimization algorithm; wind turbine

CLC number: TN925

Document code: A

Article ID: 1005-1120(2021)02-0259-12

0 Introduction

Energy is particularly important in the rapid development of society. At present, the proportion of non-renewable energy power generation is very large, causing environmental pollution and global warming. Therefore, it is of significance to develop clean and sustainable energy^[1]. In recent years, wind energy, as a clean and environmentally friendly renewable energy, has been developed rapidly^[2]. Wind energy is a kind of uncontrollable energy because of its randomness and instability. Wind turbines feature complex nonlinear dynamics under the influence of stochastic wind disturbance and gyroscopic load, and are not so easy to control. At present, studies in wind power generation mainly include maximum power point tracking (MPPT) and

reduction of mechanical stresses^[3].

The wind turbine has strong nonlinearity and uncertainty, so it is important to design a controller with strong robustness and desired dynamic characteristics. Robust control for wind turbine includes robust adaptive control^[4], fuzzy control^[5], model predictive control^[6], back-stepping control^[7], and sliding mode control (SMC)^[8]. Among these robust control methods, SMC has relatively convenient implementation and strong robustness against external disturbance and model uncertainty. To overcome the shortcomings of quasi-continuous sliding mode in convergence speed and smoothness of control action^[9], a virtual control was proposed to increase the relative order. Compared with original algorithms, faster convergence speed and smoother control ac-

*Corresponding author, E-mail address: lfxiao@nuaa.edu.cn.

How to cite this article: MA Leiming, XIAO Lingfei, SATTAROV Robert R, et al. Design of wind turbine torque controller for second-order integral sliding mode based on VGWO algorithm [J]. Transactions of Nanjing University of Aeronautics and Astronautics, 2021, 38(2): 259-270.

<http://dx.doi.org/10.16356/j.1005-1120.2021.02.007>

tion can be achieved. Saravanakumar et al.^[10] designed a wind turbine controller with fast dynamic response and high steady-state tracking accuracy to improve the utilization of wind energy. Hu et al.^[11] designed a SMC based on disturbance observer (DOB). The parameter uncertainty and wind speed randomness of wind turbine were estimated by DOB to achieve maximum wind power extraction. At the same time, to improve the utilization rate of wind energy, the actual rotor speed of wind turbine should accurately track the reference rotor speed. Nonlinear terminal sliding mode control (TSMC) can meet the requirement, but it generates chattering, which is unfavorable to the operation of wind turbines^[12]. At present, the methods of eliminating chattering mainly include the quasi-sliding mode method, the boundary layer method, the reaching law method, and the high-order sliding mode (HOSMC)^[13]. The quasi-sliding mode method, the boundary layer method and the reaching law can attenuate chattering to some extent, but they lose the invariance of SMC. HOSMC not only retains the advantages of traditional SMC, but also attenuates chattering and achieves finite time convergence.

HOSMC can be divided into the second-order sliding mode control (SOSMC) and the arbitrary order SMC. The SOSMC is widely used because of its simple structure and less required information. The most common methods are the twisting algorithm, the sub-optimal algorithm, the prescribed convergence law, and the super twisting algorithm^[14]. Among them, the twisting algorithm is the earliest proposed second-order sliding mode algorithm. Its convergence trajectory features “twisted”, and the convergence process inevitably chatters. The prescribed convergence law is to use the control law based on symbolic function in the traditional first-order SMC to make the system converge and keep on a preset sliding surface, and then make the system converge to the second-order sliding surface in a finite time, and finally realize the SOSMC. Super twisting algorithm is the only one that does not need to calculate the derivatives of sliding mode

variables and has continuous output among four SOSMC algorithms. Therefore, the super twisting algorithm has attracted the most extensive attention. A second-order sliding mode controller was proposed to reduce the fatigue load during the operation of wind turbine^[15]. Abolvafaei et al.^[16] designed a second-order fast terminal sliding mode controller by combining TSMC and PID. The better tracking effect could be guaranteed by using the PID sliding mode surface. Moreover, the model uncertainty and external disturbance were not considered, which made it difficult to highlight the robustness advantages of SMC. And a strategy of designing speed controllers based on the quasi-continuous HOSMC was proposed to ensure that the wind turbine works well in different wind modes. The influence of external disturbance and parameter uncertainty was considered^[17]. In this paper, the presented second-order integral sliding mode control (SOISMC) strategy eliminates steady-state tracking error in integral sliding mode (ISM) and reduces chattering in HOSMC. The controller has a fast convergence speed, strong robustness and effective chattering reduction.

Due to various uncertainties in the actual system, the existing SOSMC method can deal with the problem of system uncertainty, but the premise is that the upper bound of the system uncertainty must be estimated in advance before the parameters are selected. However, in practical engineering design, it is unrealistic to know the bounds of various uncertainties of the system, which leads to the difficulty in parameter selection. Besides, the SOISMC can effectively reduce chattering, but the number of adjustable parameters will increase with the increase of order. It is extremely difficult to manually adjust the controller parameters. As far, some conventional gradient-based optimizations such as Newton and interior point methods have been proposed. But these optimization methods may fail to obtain the optimal parameters due to their high dependence of the accurate system model. Hence, several heuristic algorithms have been developed to overcome the above

challenges, such as the particle swarm optimization (PSO) and the grey wolf optimization (GWO). These optimization algorithms can achieve an efficient global search with a lower dependence of the accurate system model^[18]. Typical swarm intelligence optimization algorithms include PSO^[19], GWO^[20] and the artificial bee colony (ABC)^[21]. Heuristic optimization algorithms have been widely used to solve the problems of function optimization and clustering optimization because of its simple structure and few adjusting parameters. Bekakra et al.^[22] used PSO to adjust the controller parameters to ensure the maximum wind energy extraction. The results show that the PSO can obtain better control effects than manual adjustment parameters. And differential evolution (DE) algorithm is used to improve the doubly fed induction generator performance under disturbance^[23]. Recently, GWO, inspired by the leadership and hunting methods of the grey wolves in nature, has been widely used. In GWO, the location of the prey is the solution of the corresponding problem. And it is shown that GWO is superior to PSO and genetic algorithms in searching global optimal solution^[24]. GWO has a fast convergence speed and strong local search ability. But there are some problems such as insufficient global search ability, low solution accuracy and slow convergence speed in the later stage of optimization^[20]. The main advantages of PSO are strong global search ability, simple principle and fast convergence speed. The main disadvantages are that the local search ability of the algorithm is poor and the search accuracy is low^[19]. These algorithms have their own advantages. Combining the advantages of different algorithms can achieve better results. A hybrid algorithm of GWO and DE was proposed^[25], which used GWO to improve the local search ability and used DE to improve the global search ability. The presented variable speed grey wolf optimization (VGWO) combines the strong local search ability of GWO and the fast convergence speed and strong global search ability of PSO, and realizes the parameter optimization of wind turbine torque controller.

1 Mathematical Model of Wind Turbine

In general, a wind turbine is mainly composed of an aerator (including blades, a pitch system, a hub and a yaw system), a drive-train (including main shaft bearings, the main shaft and a gearbox) and a generator, corresponding to aerodynamic, mechanical and electrical components, respectively. Fig.1 shows the structure of a wind turbine.

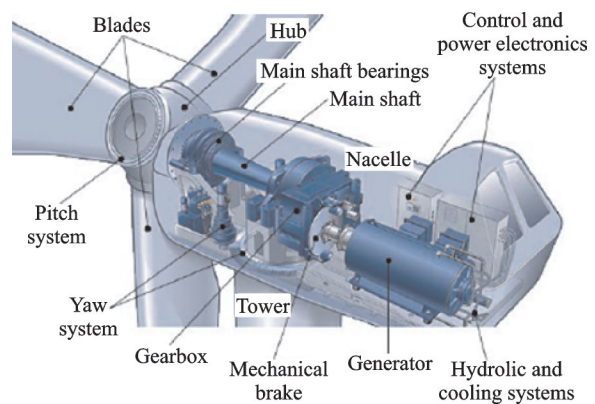


Fig.1 Typical structure of a wind turbine^[26]

The work state of a wind turbine can be divided into four parts, as shown in Fig.2. The wind turbine is in shutdown state in stage 1 and stage 4. Stage 2 is the MPPT stage. MPPT can be realized by controlling the rotation speed of the wind turbine rotor. Stage 3 is a constant power operation stage. Considering the mechanical condition of a wind turbine, constant power operation is realized by adjusting the pitch angle. This paper mainly studies that the wind turbine operates in the maximum wind energy capture stage (stage 2, as shown in Fig.2).

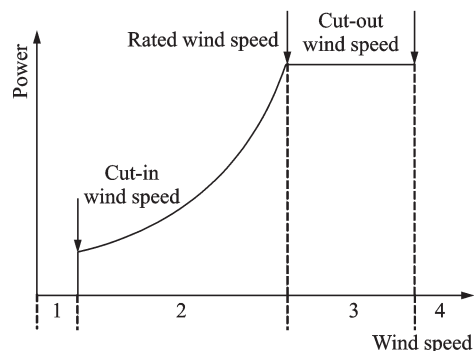


Fig.2 Power curve of wind turbine

1.1 Aerodynamics model

Eq. (1) gives the nonlinear function for wind energy capture

$$C_p = \frac{P}{0.5\rho\pi R^2 v^3} \quad (1a)$$

$$T_a = \frac{P}{\omega_r} = \frac{\rho\pi R^3 C_p v^2}{2\lambda} \quad (1b)$$

where P is the output power, C_p the power coefficient of the wind turbine, v the wind speed, ρ the air density, λ the tip speed ratio, R the wind turbine rotor radius, ω_r the rotor speed, and T_a the aerodynamic torque.

λ is defined as

$$\lambda = \frac{R\omega_r}{v} \quad (2a)$$

From Eq.(2a), we can obtain

$$\lambda_{opt} = \frac{R\omega_r^*}{v} \quad (2b)$$

where λ_{opt} denotes the best tip speed ratio, and ω_r^* the reference rotor speed.

The C_p can be expressed as follows^[27]

$$C_p(\beta, \lambda) = 0.5176 \left(\frac{116}{\lambda_i} - 0.4\beta - 5 \right) e^{-\frac{21}{\lambda_i}} + 0.0068\lambda \quad (3a)$$

$$\frac{1}{\lambda_i} = \frac{1}{\lambda + 0.08\theta} - \frac{0.035}{\theta^3 + 1} \quad (3b)$$

According to Eqs.(2,3), the change of ω_r and v will cause the change of λ and C_p . Fig.3 shows the relationship among θ , λ and C_p . With the constant pitch angle $\theta = 0^\circ$, MPPT can be achieved by changing λ and ω_r . As long as a wind turbine meets $\lambda = \lambda_{opt}$, the wind turbine can operate with C_{pmax} .

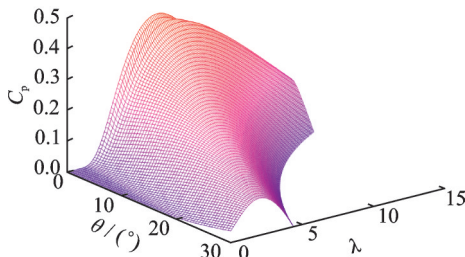


Fig.3 Power coefficient curve of wind turbine

1.2 Drive train model

Fig.4 shows a dynamic wind turbine model. The model includes a rotor and a generator, which

are modeled by two inertial models. The two-mass model is suitable for the analysis of the dynamic characteristics of wind turbines^[3,28]. In Fig.4, ω_g is the generator speed and n_g the transmission ratio, J_r and J_g are the rotor inertia and the generator inertia, respectively, D_r and D_g are the rotor external damping coefficient and the generator external damping coefficient, respectively, T_e is the generator torque, and K_{dt} , D_{dt} are the torsional stiffness and the torsional damping, respectively.

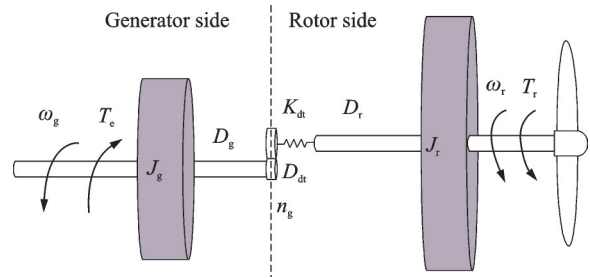


Fig.4 Model of wind turbine

Assuming the gearbox is ideal, we have $n_g\omega_r(t) = \omega_g(t)$. It gives

$$J_t \dot{\omega}_r = T_a - D_t \omega_r - n_g T_e \quad (4)$$

where $J_t = J_r + n_g^2 J_g$, $D_t = D_r + n_g^2 D_g$ are the total inertia and the total external damping coefficient of the wind turbine, respectively.

Let $A = -D_t/J_t$, $B = -n_g/J_t$ and $d = T_a/J_t$, then we have

$$\dot{\omega}_r = A\omega_r + Bu + d \quad (5)$$

where $u = T_e$.

1.3 Uncertain model of wind turbine

The parameters J_t and D_t have variations ΔJ_t and ΔD_t , respectively. Given the parameter variations, the model of the wind turbine is defined as

$$\dot{\omega}_r = (A + \Delta A)\omega_r + (B + \Delta B)u + (d + \Delta d) \quad (6a)$$

where ΔA , ΔB and Δd represent the uncertainties of A , B and d , respectively.

Let $g(t) = \Delta A\omega_r + \Delta B u + d + \Delta d$, which represents the lumped disturbance on subsystems Eq.(6a). It can be re-written as

$$\dot{\omega}_r = A\omega_r + Bu + g(t) \quad (6b)$$

Assumption 1 The lumped disturbances $g(t)$ are continuous and satisfy $\| \dot{g}(t) \| \leq D$, where D is

known positive constants.

2 Design of SOISMIC

With the wind speed changing, the rotor speed of the wind turbine can be adjusted by controlling the generator torque, so that the rotor speed of the wind turbine can track the reference rotor speed. The control schematic is shown in Fig.5.

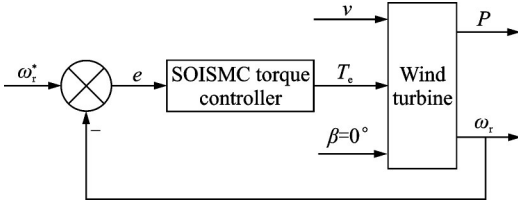


Fig.5 Principle of wind turbine torque controller

2.1 Design of sliding mode surface

The sliding mode surface is designed based on rotor speed tracking error e , and the integral term is added to eliminate the steady-state error. The first-order sliding mode surface is as follows

$$\sigma = e + \alpha \int_0^t e dt \quad (7a)$$

where α is a positive constant, and $e = \omega_r^* - \omega_r$.

The second-order sliding mode surface is as follows

$$s = \dot{\sigma} + \gamma\sigma + \beta \int_0^t \sigma dt \quad (7b)$$

where γ and β are positive numbers, which can be chosen and utilized to guarantee the convergence speed of the rotor speed tracking error.

Hence, the sliding mode manifold is

$$S = \{e | \sigma = \dot{\sigma} = \ddot{\sigma} = 0 \cap s = \dot{s} = 0\}$$

2.2 Design of torque controller

The derivation of σ is obtained

$$\begin{aligned} \dot{\sigma} &= \dot{e} + \alpha e = \dot{\omega}_r^* - \dot{\omega}_r + \alpha(\omega_r^* - \omega_r) = \\ &\dot{\omega}_r^* + \alpha(\omega_r^* - \omega_r) - A\omega_r - Bu - g(t) = \\ &\dot{\omega}_r^* + \alpha\omega_r^* - (A + \alpha)\omega_r - Bu - g(t) \end{aligned} \quad (8a)$$

The derivation of Eq.(8a) can be obtained as follows

$$\ddot{\sigma} = \ddot{e} + \alpha\dot{e} = \ddot{\omega}_r^* + \alpha\dot{\omega}_r^* - (\alpha + A)\dot{\omega}_r - B\dot{u} - \dot{g}(t) \quad (8b)$$

The derivation of s is obtained

$$\dot{s} = \ddot{\sigma} + \gamma\dot{\sigma} + \beta\sigma \quad (9)$$

By substituting Eq.(8) into Eq.(9), we have

$$\dot{s} = \ddot{\omega}_r^* + \alpha\dot{\omega}_r^* - (\alpha + A)\dot{\omega}_r - B\dot{u} - \dot{g}(t) + \gamma\dot{\sigma} + \beta\sigma$$

The control law u is as follows

$$u = u_{eq} + u_{sw} \quad (10a)$$

Overlook the uncertainty and disturbance, the equivalent control law u_{eq} is as follows

$$\dot{u}_{eq} = B^{-1}[\ddot{\omega}_r^* + \alpha\dot{\omega}_r^* - (\alpha + A)\dot{\omega}_r + \gamma\dot{\sigma} + \beta\sigma] \quad (10b)$$

The switching control law u_{sw} is as follows

$$\dot{u}_{sw} = B^{-1}[k_{s1}s + k_{s2}\text{sgn}(s)] \quad (10c)$$

where both k_{s1} and k_{s2} are position numbers.

Let $\varphi = \ddot{\omega}_r^* + \alpha\dot{\omega}_r^* - (\alpha + A)\dot{\omega}_r + \gamma\dot{\sigma} + \beta\sigma$ and $\psi = k_{s1}s + k_{s2}\text{sgn}(s)$, then we have

$$u = \int_0^t B^{-1}(\varphi + \psi) dt \quad (11)$$

2.3 Stability analysis

Theorem 1 The wind turbine subsystem given by Eq. (6) converges asymptotically under the SOISMIC of Eq. (7), with sliding mode controller of Eq.(11), if Eq.(12) is held.

$$k_{s2} > D \quad (12)$$

Proof Choose the following Lyapunov function

$$V = \frac{1}{2}s^2$$

The derivation of Lyapunov function is obtained

$$\begin{aligned} \dot{V} &= s\dot{s} = \\ s[\ddot{\omega}_r^* + \alpha\dot{\omega}_r^* - (\alpha + A)\dot{\omega}_r - B\dot{u} - \dot{g}(t) + \gamma\dot{\sigma} + \\ &\beta\sigma] = -sk_{s1}s - sk_{s2}\text{sgn}(s) - s\dot{g}(t) \end{aligned}$$

According to Assumption 1, it gives

$$\begin{aligned} \dot{V} &= s\dot{s} \leq -sk_{s1}s - sk_{s2}\text{sgn}(s) + \|s\| \cdot D = \\ &-k_{s1}\|s\|^2 - (k_{s2} - D)\|s\| \end{aligned} \quad (13)$$

From $k_{s1} > 0$ and $k_{s2} > D$, we have

$$\dot{V} < 0$$

The proof is completed.

3 Parameter Optimization Based on VGWO

Combining the advantages of different algorithms to construct a new hybrid algorithm is an important research direction of current algorithm im-

provement. In this paper, VGWO with a fast convergence speed, high solution accuracy and strong global search ability is proposed, which combines strong local search ability of GWO and fast convergence speed and strong global search ability of PSO. The VGWO introduces the velocity component of

PSO into GWO. The velocity component includes inertia, social and perceptual components. The velocity component in GWO can not only avoid prematurity but also accelerate the convergence speed. The SOISM control structure for the wind turbine is shown in Fig.6.

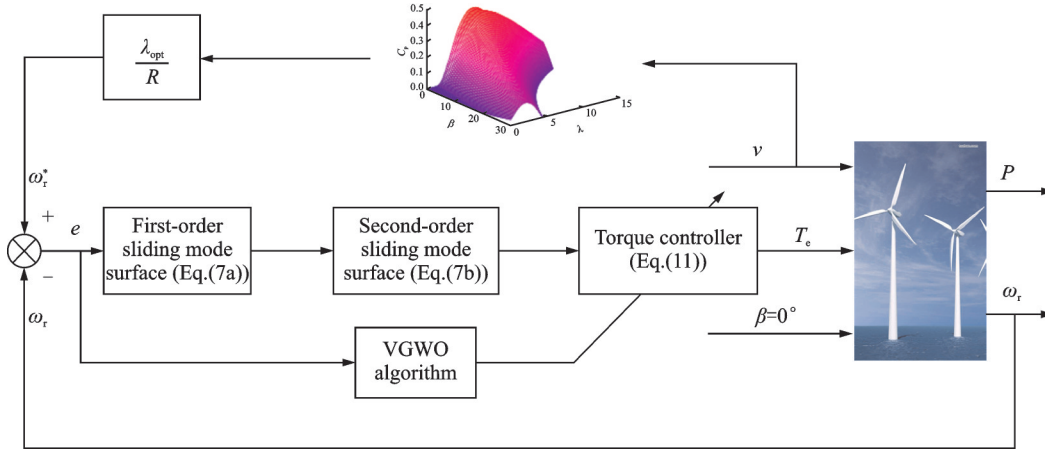


Fig.6 The proposed control structure for the wind turbine

3.1 Principle of GWO

GWO is a new heuristic algorithm, which imitates the dominance and hunting style of grey wolves in nature. According to the fitness value, we consider the position of alpha (α_{GWO}) as the optimal solution. Consequently, the positions of beta (β_{GWO}) and delta (δ_{GWO}) are considered as the second and the third best solutions, respectively. The position of omega (ω_{GWO}) are assumed to be candidate solutions. In GWO, the optimization is guided by α_{GWO} , β_{GWO} , δ_{GWO} and ω_{GWO} . The ω_{GWO} wolves follow the other three wolves. The specific steps of the VGWO algorithm are as follows

$$\begin{cases} A_{GWO} = 2a \cdot r_1 - a \\ C_{GWO} = 2r_2 \end{cases} \quad (14)$$

$$\begin{cases} D_{GWO} = |C_{GWO} \cdot X_p(k) - X(k)| \\ X(k+1) = X_p(k) - A_{GWO} \cdot D_{GWO} \end{cases} \quad (15)$$

$$\begin{cases} X_1 = X_\alpha - A_1 |C_1 \cdot X_\alpha - X| \\ X_2 = X_\beta - A_2 |C_2 \cdot X_\beta - X| \\ X_3 = X_\delta - A_3 |C_3 \cdot X_\delta - X| \end{cases} \quad (16)$$

$$X(k+1) = \frac{X_1 + X_2 + X_3}{3} \quad (17)$$

where k indicates the current iteration, D_{GWO} the dis-

tance between grey wolf and prey, X_p the position vector of the prey, X the position vector of current grey wolf, a is linearly decreased in $[0, 2]$, A_{GWO} and C_{GWO} are the coefficient vectors, r_1, r_2 the random vectors in $[0, 1]$; X_1, X_2, X_3 the distance vectors of ω_{GWO} relative to α_{GWO} , β_{GWO} , and δ_{GWO} , respectively; $A_1, A_2, A_3, C_1, C_2, C_3$ the coefficients..

3.2 Improvement of GWO

The particles of PSO can memorize the best position they found and the distance and direction of flight are determined by the velocity of each particle. The speed can be adjusted dynamically based on the flight experience of itself and its companions. Therefore, PSO has a faster convergence speed and stronger global search capability.

$$\begin{aligned} v_i(k+1) &= \zeta \times v_i(k) + c_1 \text{random}(0,1) \times \\ &(X_1 - x_i(k)) + c_2 \text{random}(0,1) \times (X_2 - x_i(k)) + \\ &c_3 \text{random}(0,1) \times (X_3 - x_i(k)) \end{aligned} \quad (18)$$

$$x_i(k+1) = x_i(k) + v_i(k+1) \quad (19)$$

where ζ is the inertial factor, v_i the grey wolf speed, x_i the current position of the grey wolf, and $c_1 = c_2 = c_3 = 0.5$ are the learning factors.

The pseudo code of the VGWO algorithm is shown in Table 1, where X_α , X_β and X_δ repre-

sent the positions of α_{GWO} , β_{GWO} and δ_{GWO} , respectively. The size of the grey wolf population is set to 30 and the maximum number of iterations is set to 100.

Table 1 Pseudo code of the VGWO algorithm

1. Initialize the grey wolf population $X_i (i = 1, 2, \dots, n)$ by Eq.(15)
2. Initialize a , A_{GWO} and C_{GWO} by Eq.(14)
3. Calculate the fitness of each search agent
 X_α = the best search agent
 X_β = the second best search agent
 X_δ = the third best search agent
4. While ($k < \text{max number of iterations}$)
5. For each search agent
6. Update the position of the current search agent by Eqs.(16–19)
7. End For
8. Update a , A_{GWO} and C_{GWO} by Eq.(14)
9. Calculate the fitness of all search agents
10. Update X_α , X_β and X_δ
 $k = k + 1$
11. End While
12. Return X_α

To optimize the parameters by using performance indexes, the fitness function of the integral absolute error (IAE) is designed as

$$\text{Minimize } J = \int_0^t |e(t)| dt \quad (20)$$

4 Simulation and Analysis

The proposed control structure for the wind turbine is shown in Fig.6. The simulation in this paper includes three aspects. Firstly, the optimization results based on PSO, GWO and VGWO optimization algorithms are given. Secondly, the simulation is carried out under SOISMIC. Finally, considering the model uncertainty and external disturbance, the proposed SOISMIC and ISMC are compared and simulated. The wind turbine parameters are given in Table 2.

The wind speed simulation is shown in Fig.7. Wind speed model includes basic wind, random wind, gust and gradual wind. The basic wind is 7 m/s, the holding time is 400 s and the sampling

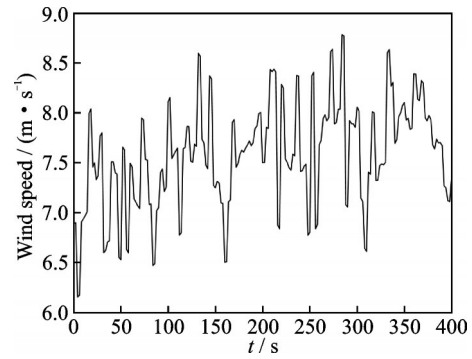


Fig.7 Wind speed

Table 2 Parameters of wind turbine

Parameter	Value
R/m	21.65
ρ/m^3	1.308
$J_r/(kg \cdot m^2)$	325 000
$J_g/(kg \cdot m^2)$	34.4
$D_r/[(N \cdot m) \cdot (rad \cdot s)^{-1}]$	45.52
$D_g/[(N \cdot m) \cdot (rad \cdot s)^{-1}]$	0.4
n_g	43.165

time of the random wind is 2 s.

4.1 Comparison of optimization algorithms

Fig.8 is the 3D graph of universal standard functions. In this paper, the function is used to test the performance of PSO, GWO and VGWO briefly.

Fig.9 shows the performance comparison of PSO, GWO and VGWO. It can be seen that the optimal value of VGWO is the minimum, and its adjustment time is shorter than that of GWO. The simulation result shows that VGWO combines the fast convergence speed of PSO and the effectiveness of GWO. Thus, it has a better optimization performance.

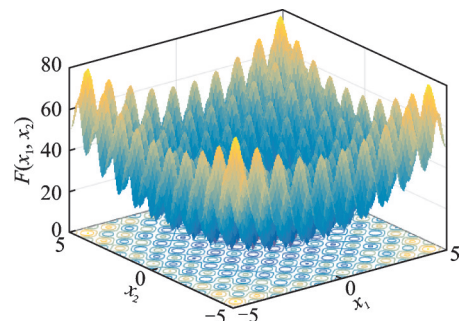


Fig.8 Universal standard functions

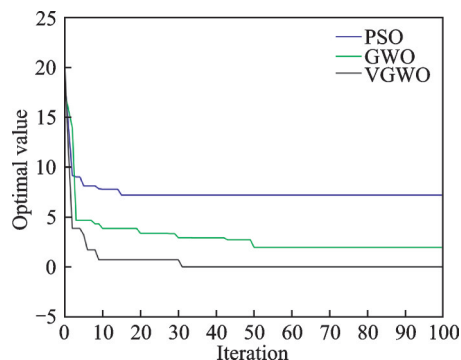


Fig.9 Performance comparison of PSO, GWO and VGWO

4.2 Robustness simulation

In order to show the robustness of the present method in this paper, the following two cases are considered.

Case 1 $\Delta A = 0, \Delta B = 0, \Delta d = 0$.

Case 2 $\Delta A = 10\%A, \Delta B = 10\%B, \Delta d = \sin(\pi t/125)$.

To illustrate the validity, we conduct a comparative study between the proposed SOISM and ISMC. The expression of ISMC is as follows

$$u = B^{-1} [\dot{\omega}_r^* + \alpha \omega_r^* - (\alpha + A) \omega_r + k_{s1} s + \epsilon_{s2} \operatorname{sgn}(s)]$$

where ISMC controller parameters are shown in Table 3.

Table 3 Optimization results based on VGWO

Method		ISMC	SOISM
IAE		42.078 2	37.768 1
α	Range	0—2	0—2
	Result	1.354 3	1.185 1
β	Range		0—1
	Result		0.001 0
γ	Range		0—0.5
	Result		0.028 3
k_{s1}	Range	0—0.5	0—0.5
	Result	0.309 6	0.001 0
k_{s2}	Range	0—1.5	0—1.5
	Result	0.286 4	0.001 0

(1) Case 1

Fig.10 shows the comparison of fitness function for SOISM and ISMC based on the VGWO optimization algorithm. It can be seen that the fitness function value based on SOISM is smaller

than that of ISMC. The result shows that SOISM has a better control effect than ISMC. Fig.11 shows that the rotor speed based on the proposed SOISM has higher tracking accuracy, where e_ω is the rotor speed error. Fig.12 and Fig.13 show that the proposed SOISM can effectively reduce chattering, which reduces the fatigue load of generator and prolong the service life. Fig.14 and Fig.15 show that the proposed SOISM has higher C_p and P , where C_p^* is the reference power coefficient of the wind turbine.

The data in Figs.11—13 are further processed and then shown in Tables 4—6, respectively. $\operatorname{Min}(\cdot)$,

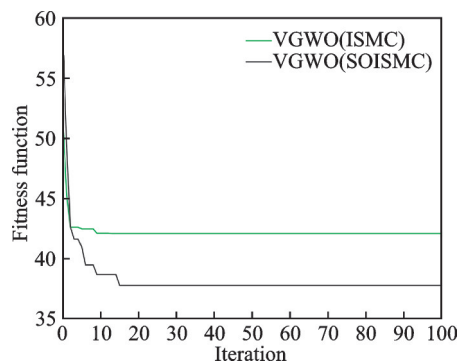


Fig.10 Comparison of fitness function

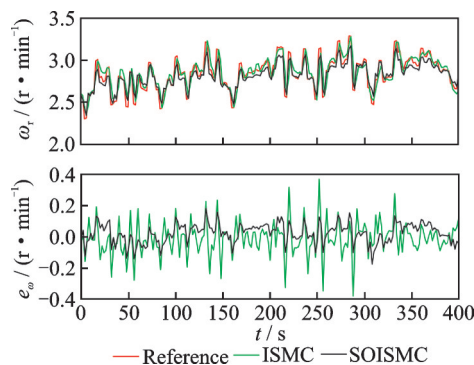


Fig.11 Rotor speed for Case 1

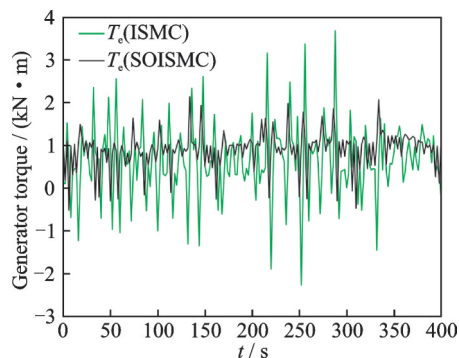


Fig.12 Generator torque for Case 1

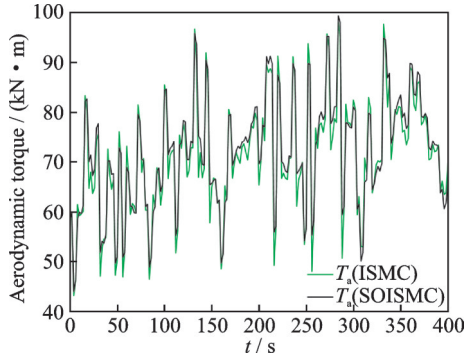


Fig.13 Aerodynamic torque for Case 1

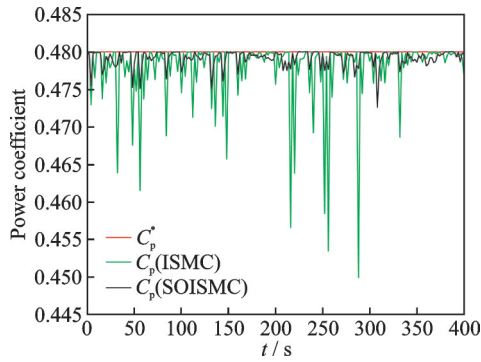


Fig.14 Power coefficient for Case 1

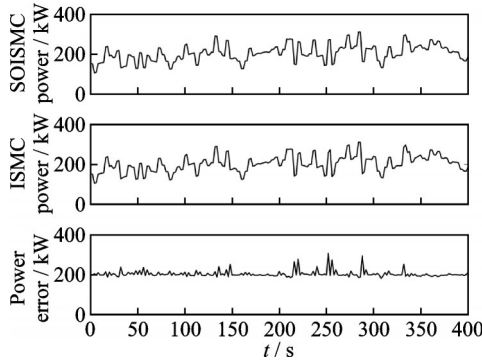


Fig.15 Power for Case 1

$\text{Max}(\cdot)$, $\text{Mean}(\cdot)$ and $\text{STDEV}(\cdot)$ represent the minimal, the maximal, the mean and the standard deviation of the corresponding variables, respectively. It can be seen from the tables that the standard deviation of SOISM is less than that of ISM. It shows that the operation of the wind turbine with SOISM control strategy is more stable.

Table 4 Comparison of rotor speed error for Case 1

Method	Min(\cdot)	Max(\cdot)	Mean(\cdot)	STDEV(\cdot)
ISM	-0.382 8	0.368 9	-0.010 8	0.106 7
SOISM	-0.175 6	0.181 9	0.022 8	0.063 8

Table 5 Comparison of generator torque for Case 1

Method	Min(\cdot)	Max(\cdot)	Mean(\cdot)	STDEV(\cdot)
ISM	-2.275 0	3.685 4	0.632 4	0.835 8
SOISM	-0.522 0	2.133 2	0.897 7	0.436 1

Table 6 Comparison of aerodynamic torque for Case 1

Method	Min(\cdot)	Max(\cdot)	Mean(\cdot)	STDEV(\cdot)
ISM	43.105 3	98.000 7	70.945 5	11.570 6
SOISM	43.909 9	99.286 2	71.920 3	11.471 3

(2) Case 2

Figs.16—20 show the case in which the same model uncertainty 10% and external disturbance $\Delta d = \sin(\pi t/125)$ are considered. Compared with Case 1, the system uncertainty is considered in Case 2. ISM control performance deteriorates compared with SOISM. It shows that SOISM can effectively weaken system chattering and improve the convergence speed. The conclusion is similar to Case 1. The data in Figs.16—18 are further processed and then shown in Tables 7—9, respectively. It can be seen from the tables that SOISM has stronger robustness to external disturbance and model uncertainty.

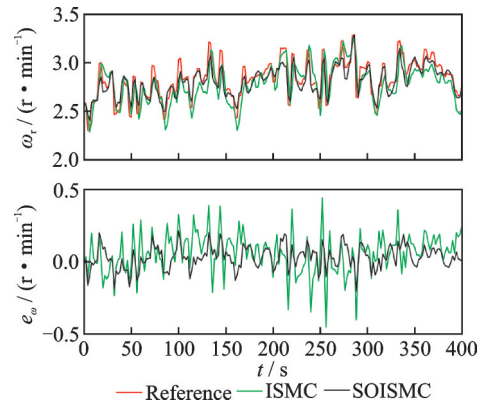


Fig.16 Rotor speed for Case 2

5 Conclusions

Based on the model uncertainty and external disturbance, a robust control method based on VGWO for wind turbines is proposed. The VGWO algorithm is used to adjust the parameters of the sliding mode controller. The proposed method is proved mathematically and simulated in Matlab/

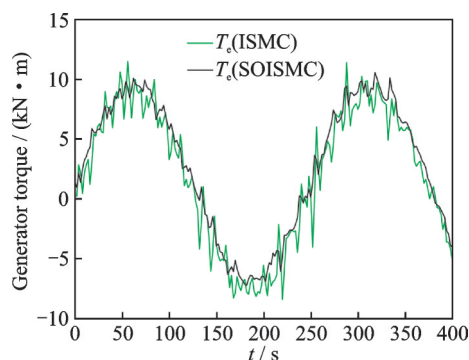


Fig.17 Generator torque for Case 2

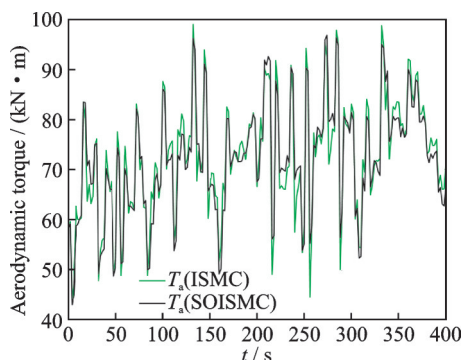


Fig.18 Aerodynamic torque for Case 2

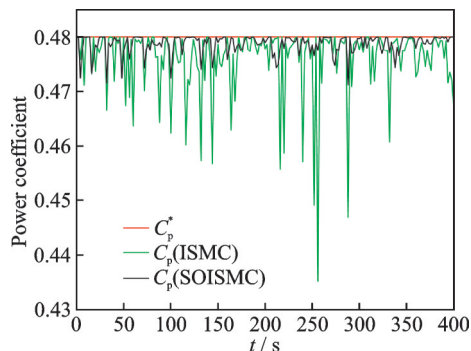


Fig.19 Power coefficient for Case 2

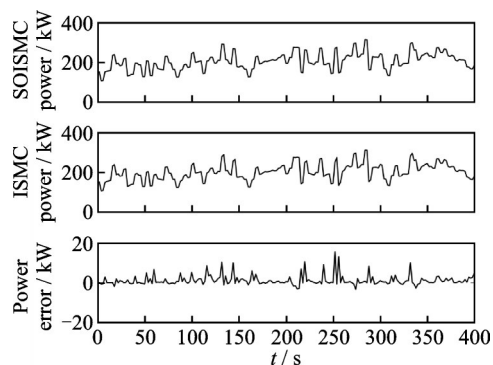


Fig.20 Power for Case 2

Simulink, which provides a strong theoretical background for the application of the SOISM method for wind turbines. Simulation results show that SO-

Table 7 Comparison of rotor speed error for Case 2

Method	Min(\cdot)	Max(\cdot)	Mean(\cdot)	STDEV(\cdot)
ISM	-0.454 6	0.441 5	0.057 8	0.135 9
SOISM	-0.205 3	0.213 4	0.029 3	0.079 9

Table 8 Comparison of generator torque for Case 2

Method	Min(\cdot)	Max(\cdot)	Mean(\cdot)	STDEV(\cdot)
ISM	-8.410 2	11.502 6	2.112 0	5.652 3
SOISM	-7.233 8	10.573 1	2.828 6	5.469 2

Table 9 Comparison of aerodynamic torque for Case 2

Method	Min(\cdot)	Max(\cdot)	Mean(\cdot)	STDEV(\cdot)
ISM	43.988 4	98.970 2	72.436 7	11.655 1
SOISM	42.944 1	96.868 5	72.033 4	11.550 6

ISM has a fast convergence speed and strong robustness, and it can effectively weaken system chattering compared with ISM. Besides, VGWO has a fast convergence speed, high accuracy and strong global search ability. The presented wind turbine torque controller effectively realizes maximum wind power extraction for wind turbines, which meets the control requirements. In the future study, the upper bound of disturbance should be estimated by the adaptive law, and the actuator fault should be considered.

References

- [1] ABDELMALEK S, AZAR A T, DIB D. A novel actuator fault-tolerant control strategy of DFIG-based wind turbines using Takagi-Sugeno multiple models[J]. International Journal of Control, Automation and Systems, 2018, 16(3): 1415-1424.
- [2] FOLEY A M, ÓGALLACHÓIR B P, MCKEOGH E J, et al. Addressing the technical and market challenges to high wind power integration in Ireland[J]. Renewable and Sustainable Energy Reviews, 2013, 19: 692-703.
- [3] AZIZI A, NOURISOLA H, SHOJA-MAJIDABAD S. Fault tolerant control of wind turbines with an adaptive output feedback sliding mode controller[J]. Renewable Energy, 2019, 135: 55-65.
- [4] YADAV A K, PATHAK P K, SAH S V, et al. Sliding mode-based fuzzy model reference adaptive control technique for an unstable system[J]. Journal of The Institution of Engineers (India) : Series B, 2019, 100(2): 169-177.

- [5] GIANNAKIS A, KARLIS A, KARNAVAS Y L. A combined control strategy of a DFIG based on a sensorless power control through modified phase-locked loop and fuzzy logic controllers[J]. *Renewable Energy*, 2018, 121: 489-501.
- [6] MAHMOUD M S, OYEDEJI M O. Adaptive and predictive control strategies for wind turbine systems: a survey[J]. *IEEE/CAA Journal of Automatica Sinica*, 2019, 6(2): 364-378.
- [7] YIN X, LIN Y, LI W, et al. Adaptive back-stepping pitch angle control for wind turbine based on a new electro-hydraulic pitch system[J]. *International Journal of Control*, 2015, 88(11): 2316-2326.
- [8] BELTRAN B, BENBOUZID M E H, AHMED-ALI T. Second-order sliding mode control of a doubly fed induction generator driven wind turbine[J]. *IEEE Transactions on Energy Conversion*, 2012, 27(2): 261-269.
- [9] FAN J S, ZHANG H X, WANG G M, et al. Improvement of higher order sliding mode control and its application[J]. *Control and Decision*, 2011, 26(9): 1436-1440.
- [10] SARAVANAKUMAR R, JENA D. Validation of an integral sliding mode control for optimal control of a three blade variable speed variable pitch wind turbine[J]. *International Journal of Electrical Power & Energy Systems*, 2015, 69: 421-429.
- [11] HU Z, WANG J, MA Y, et al. Research on speed control system for fixed-pitch wind turbine based on disturbance observer[C]//*Proceedings of 2009 World Non-Grid-Connected Wind Power and Energy Conference*. Nanjing, China: IEEE, 2009: 221-225.
- [12] FENG Y, YU X, HAN F. On nonsingular terminal sliding-mode control of nonlinear systems[J]. *Automatica*, 2013, 49(6): 1715-1722.
- [13] XIANG W, HUANGPU Y. Second-order terminal sliding mode controller for a class of chaotic systems with unmatched uncertainties[J]. *Communications in Nonlinear Science and Numerical Simulation*, 2010, 15(11): 3241-3247.
- [14] LEVANT A. Sliding order and sliding accuracy in sliding mode control[J]. *International Journal of Control*, 1993, 58(6): 1247-1263.
- [15] MÉRIDA J, AGUILAR L T, DÁVILA J. Analysis and synthesis of sliding mode control for large scale variable speed wind turbine for power optimization[J]. *Renewable Energy*, 2014, 71: 715-728.
- [16] ABOLVAFAEI M, GANJEFAR S. Maximum power extraction from a wind turbine using second-order fast terminal sliding mode control[J]. *Renewable Energy*, 2019, 139: 1437-1446.
- [17] JING Y, SUN H, ZHANG L, et al. Variable speed control of wind turbines based on the quasi-continuous high-order sliding mode method[J]. *Energies*, 2017, 10(10): 1626.
- [18] ZHANG Y, GONG D, GENG N, et al. Hybrid barebones PSO for dynamic economic dispatch with valve-point effects[J]. *Applied Soft Computing*, 2014, 18: 248-260.
- [19] GAO W, LIU S, HUANG L. Particle swarm optimization with chaotic opposition-based population initialization and stochastic search technique[J]. *Communications in Nonlinear Science and Numerical Simulation*, 2012, 17(11): 4316-4327.
- [20] MIRJALILI S, MIRJALILI S M, LEWIS A. Grey wolf optimizer[J]. *Advances in Engineering Software*, 2014, 69: 46-61.
- [21] CONG T D, ZHIJIAN W, ZELIN W, et al. A novel hybrid data clustering algorithm based on artificial bee colony algorithm and K-means[J]. *Chinese Journal of Electronics*, 2015, 24(4): 694-701.
- [22] BEKAKRA Y, ATTOUS D B. Optimal tuning of PI controller using PSO optimization for indirect power control for DFIG based wind turbine with MPPT[J]. *International Journal of System Assurance Engineering and Management*, 2014, 5(3): 219-229.
- [23] SURYOATMOJO H, ZAKARIYA A M B, ANAM S, et al. Optimal controller for doubly fed induction generator (DFIG) using differential evolutionary algorithm[C]//*Proceedings of 2015 International Seminar on Intelligent Technology and Its Applications*. Surabaya, Indonesia: IEEE, 2015.
- [24] ZHANG X M, TU Q, KANG Q, et al. Hybrid optimization algorithm based on grey wolf optimization and differential evolution for function optimization[J]. *Computer Science*, 2017, 44(9): 93-98.
- [25] ZHU A J, XU C P, ZHI L, et al. Hybridizing grey wolf optimization with differential evolution for global optimization and test scheduling for 3D stacked SoC[J]. *Journal of Systems Engineering and Electronics*, 2015, 26(2): 317-328.
- [26] GENG H, YANG G. Output power control for variable-speed variable-pitch wind generation systems[J]. *IEEE Transactions on Energy Conversion*, 2010, 25(2): 494-503.
- [27] LIU X, HAN Y, WANG C. Second-order sliding

mode control for power optimization of DFIG based variable speed wind turbine[J]. IET Renewable Power Generation, 2016, 11(2): 408-418.

- [28] TCHAKOUA P, WAMKEUE R, OUHROUCHE M, et al. Wind turbine condition monitoring: State-of-the-art review, new trends, and future challenges[J]. Energies, 2014, 7(4): 2595-2630.

Acknowledgements This work was supported by the National Natural Science Foundation of China (No. 51876089) and the Fundamental Research Funds for the Central Universities (No. kfjj20190205).

Authors Mr. MA Leiming is currently a postgraduate at College of Energy and Power Engineering, Nanjing University of Aeronautics and Astronautics. He has won the national scholarship, excellent paper award of Jiangsu energy forum and Triple-A student of Jiangsu. His research interest is sliding mode theory and fault tolerant control for complex systems.

Dr. XIAO Lingfei currently holds the position of associate professor within the Jiangsu Province Key Laboratory of Aerospace Power Systems, Nanjing University of Aeronautics and Astronautics. She received her Ph. D. degree from Zhejiang University in 2008. Her main research interest lies in the advanced control theory and application in complex mechanical and electrical systems, and aircraft engine systems.

Author contributions Mr. MA Leiming designed the study, compiled the models, conducted the analysis, interpreted the results, and wrote the manuscript. Dr. XIAO Lingfei contributed to data and model components for the wind turbine model. Dr. SATTAROV Robert R contributed to the discussion and background of the study. Mr. HUANG Xinhao polished up the English. All authors commented on the manuscript draft and approved the submission.

Competing interests The authors declare no competing interests.

(Production Editor: ZHANG Huangqun)

基于 VGWO 算法的风力机二阶积分滑模转矩控制器设计

马磊明¹, 肖玲斐¹, SATTAROV Robert R², 黄欣浩¹

(1. 南京航空航天大学能源与动力学院, 南京 210016, 中国; 2. 乌法国立航空技术大学机电系, 乌法, 俄罗斯)

摘要:提出了一种基于变速灰狼优化算法(Variable speed grey wolf optimization, VGWO)的二阶积分滑模(Second-order integral sliding mode control, SOISM)鲁棒控制策略。该策略的目的是实现风力机的最大风能捕获, 提高风力机的发电量。首先,根据风力机的不确定性模型,设计了一种收敛速度快、鲁棒性强且能有效抑制抖振的二阶积分滑模转矩控制器,保证了转矩控制器能够有效地跟踪参考转速。其次,考虑到灰狼优化算法(Grey wolf optimization, GWO)具有较强的局部搜索能力和粒子群优化算法(Particle swarm optimization, PSO)具有较快的收敛速度和较强的全局搜索能力,将PSO的速度分量引入GWO中,使改进的VGWO具有较快的收敛速度、较高的求解精度和较强的全局搜索能力。然后,利用VGWO对风力机转矩控制器的参数进行优化。最后,在Simulink/SimPowerSystem平台上进行了仿真,结果表明了该策略在存在外部干扰和模型不确定性情况下的有效性。

关键词:积分滑模;二阶滑模;最大功率点跟踪;优化算法;风力机